Response to RC1

Title: "Stoichiometric deviation and regulatory mechanisms of AOU-nutrient ratio in the oligotrophic Northwest Pacific Ocean"

In this document, we present the response to Referee's comments repeated in blue.

From the observed AOU/nutrient ratios, the deviations from the classical Redfield stoichiometry are actually relatively modest. Nevertheless, the authors provide a detailed mechanistic interpretation of these subtle deviations from multiple perspectives, particularly focusing on TEP production and microbial metabolic strategies. In my opinion, this represents an interesting and worthwhile attempt.

The central hypothesis proposed by the authors is that strong stratification in the TNWP leads to chronic nutrient limitation in surface waters, which promotes the production of carbon-rich TEP by phytoplankton. Subsequently, microbial communities selectively degrade nitrogen- and phosphorus-rich organic components while preferentially regenerating phosphorus, resulting in nutrient regeneration exceeding organic carbon oxidation and ultimately producing AOU/nutrient ratios slightly lower than the classical Redfield values.

From the apparent regression slopes, however, the AOU/nutrient ratios reported here are substantially higher than those previously reported by Zhu et al. in the northern South China Sea (e.g., AOU/DIN = 3.09 in Zhu et al. versus 6.28 in the present study). In my view, these represent two fundamentally different scenarios. The extremely low ratios observed by Zhu et al. were likely dominated by physical processes such as water-mass mixing, whereas the present study represents a typical open-ocean environment where biogeochemical processes are expected to play a much more important role.

TEP itself is a carbon-rich, nitrogen- and phosphorus-poor organic material. From the perspective of remineralization, degradation of TEP consumes oxygen but releases relatively little nitrogen and phosphorus. Consequently, TEP degradation would be expected to increase,

rather than decrease, the AOU/nutrient ratios relative to the Redfield expectation. Therefore, the degradation of TEP alone does not appear to support the mechanism proposed in this manuscript.

In contrast, from the perspective of TEP production, the mechanism is much more convincing. TEP production originates from phytoplankton photosynthesis, during which oxygen is produced and carbon is fixed, whereas the associated consumption of nitrogen and phosphorus is substantially lower than predicted by the Redfield ratio because of the high C:N composition of TEP. Under this scenario, AOU decreases whereas nutrient concentrations decrease much less than expected, potentially leading to relatively low AOU/nutrient ratios. Therefore, it seems reasonable that phytoplankton production of TEP could contribute to reduced AOU/nutrient ratios within the euphotic zone, or approximately the upper 0–300 m where active photosynthesis occurs.

Overall, I consider the attempt to explain the reduced AOU/nutrient ratios in the upper ocean from the perspective of TEP production to be novel and potentially important. My major comments and concerns are as follows:

Thank you very much for taking the time to review our manuscript and for providing insightful and constructive comments. Your feedback has been invaluable in helping us identify areas for improvement and in enhancing the overall quality of our work. We have carefully considered each of your suggestions and have made corresponding revisions to the manuscript. Below, we provide detailed point-by-point responses to all comments.

Major comments:

1. Use and interpretation of preformed nutrients

The use of preformed nitrate ($PreNO_3$) and preformed phosphate ($PrePO_4$) requires additional caution. The classical concept of preformed nutrients is based on the assumption that organic matter remineralization and nutrient regeneration follow a prescribed stoichiometric relationship, typically the Redfield ratio (or a fixed empirical remineralization stoichiometry). However, the central premise of the present manuscript is precisely that organic matter remineralization in the study region deviates from the classical Redfield stoichiometry. This

creates a potential inconsistency between the methodological assumptions and the scientific conclusions.

For this reason, I do not suggest removing the calculations of $PreNO_3$ and $PrePO_4$, as they may still serve as useful diagnostic residuals. However, I recommend avoiding interpreting them as the true "preformed nutrients." Instead, they should be presented as residual indicators derived under a predefined remineralization stoichiometry. Otherwise, there is a risk of circular reasoning: the manuscript uses preformed nutrients calculated under an assumed stoichiometric relationship to demonstrate that the remineralization stoichiometry itself deviates from that assumption. This logical issue should be explicitly acknowledged and discussed.

In addition, the manuscript adopts the modified approach proposed by Letscher and Villareal by introducing different remineralization coefficients for DOM and POM, which is intended to improve the realism of the calculations. This is good. Nevertheless, the parameters used in the calculations (f_{DOM}, f_{POM}, r_{DOM}, and r_{POM}) remain empirical assumptions rather than values constrained by observations from the study region. In particular, Table 1 lists multiple candidate values of r_{POM}, yet the manuscript does not explain which value was ultimately adopted or the criteria used for selecting among them. Consequently, the calculated $PreNO_3$ and $PrePO_4$ are highly dependent on these empirical parameterizations and therefore should not be regarded as independent evidence supporting the proposed mechanism responsible for the low AOU/nutrient ratios. Rather, they should be interpreted as model-dependent diagnostic quantities whose uncertainties deserve further discussion.

Response: We thank the reviewer for this important comment. We agree that the original terminology overstated the physical meaning and evidential independence of the calculated quantities. Because the residual calculation defines a reference state using prescribed remineralization parameters, a nonzero residual indicates a departure from that parameterization but is not a model independent estimate of the true preformed nutrient concentration or independent evidence of the underlying mechanism. We have therefore revised the terminology, uncertainty reporting, and interpretation throughout the manuscript.

$PreNO_3$ and $PrePO_4$ are now consistently presented as residual preformed nitrate ($rPreNO_3$) and residual preformed phosphate ($rPrePO_4$), which are diagnostic residuals that depend on the prescribed parameters. Section 2.3 has been renamed "Calculation of $rPreNO_3$ and $rPrePO_4$." Following the uncertainty treatment of Smyth and Letscher (2023), f_{DOM} and f_{POM} were each evaluated at 0.4, 0.5, and 0.6, and r_{POM} was assigned values of 6.9, 8.75, and 10.6 (Table 1/Revised Table S2). All combinations produced 27 calculations for each observation, while r_{DOM} was fixed according to the depth or density interval. Thus, no single r_{POM} value was selected. For every observation, the 27 results were summarized as minimum–maximum (arithmetic average ± standard deviation). The arithmetic average was used in the figures and interpretation, whereas the minimum, maximum, and standard deviation describe sensitivity to the prescribed parameter combinations rather than measurement or sampling uncertainty. These summaries have been deposited in the public Figshare data set (Tian, 2026; https://doi.org/10.6084/m9.figshare.31841125), allowing direct assessment of parameter dependence. We also clarify that ensemble averaging does not remove this dependence and that the 27 calculations are not interpreted as independently validated local parameter sets.

The revised method is as follows (Revised manuscript, lines 215-222):

"***2.3 Calculation of $rPreNO_3$ and $rPrePO_4$***

$rPreNO_3$ and $rPrePO_4$ were calculated using the modified formulation of Letscher and Villareal (2018), with parameter sensitivity evaluated following Smyth and Letscher (2023). For each observation, 27 calculations were performed using the prescribed DOM and POM parameter combinations. The arithmetic mean was used as the reported diagnostic value, whereas the minimum, maximum, and standard deviation describe sensitivity to the prescribed parameters. Full equations and parameter values are provided in Supplementary Method 2."

The calculation method is described in detail as follows (Supplementary materials, lines 38-64):

"*$rPreNO_3$ was computed as:*

$$rPreNO_3 = NO_{3meas} - (f_{DOM} \bullet \frac{AOU}{r_{DOM}} + f_{POM} \bullet \frac{AOU}{r_{POM}}) \quad (2),$$

where measured nitrate (NO_{3meas}) is defined as the sum of the concentrations of NO_3-N and NO_2-N. AOU is given by:

$$AOU = DO_{sat} - DO_{meas} \quad (3),$$

where DO_{sat} is the saturated DO concentration at a given temperature, salinity, and pressure (Garcia and Gordon, 1992), and DO_{meas} is the measured DO concentration. f_{DOM} and f_{POM} represent the fractions of total oxygen consumption attributed to DOM and POM, respectively. r_{DOM} and r_{POM} denote the moles of O_2 consumed per mole of nitrogen regenerated during DOM and POM remineralization, respectively. f_{DOM} and f_{POM} were each evaluated at 0.4, 0.5, and 0.6 (0.5 ± 0.1), while r_{POM} was assigned values of 6.9, 8.75, and 10.6, representing the minimum, Redfield, and maximum estimates reported in the literature (Table S2) (Letscher and Villareal, 2018; Smyth and Letscher, 2023). All combinations produced 27 calculations for each observation. These calculations were used to represent the uncertainty associated with applying empirical parameters to the broader Pacific Ocean. For each observation, the 27 estimates were summarized as minimum–maximum (arithmetic average ± standard deviation). The arithmetic average was used as the central diagnostic value in the manuscript, whereas the minimum, maximum, and standard deviation describe sensitivity to the prescribed parameter combinations. The complete summaries are available in the public data set (Tian, 2026).

Similarly, $rPrePO_4$ was computed as:

$$rPrePO_4 = PO_{4meas} - \frac{1}{16}(f_{DOM} \bullet \frac{AOU}{r_{DOM}} + f_{POM} \bullet \frac{AOU}{r_{POM}}) \quad (4)$$

Because the remineralization parameters specific to phosphorus could not be independently constrained, the nitrogen regeneration terms derived from DOM and POM were converted to phosphorus equivalents using an N:P ratio of 16:1 (Letscher and Villareal, 2018)."

Table 1/Revised Table S2. Parameters for the calculation of residual PreNO3/PrePO4 in the Pacific Ocean

Depth (m)/neutral density (γ_n)	f_{DOM}	f_{POM}	r_{POM}	r_{DOM}
0−100 m/γ_n: 24.2−24.7	0.5±0.1	0.5±0.1	6.9, 8.75, 10.6	18.1
γ_n> 24.7	0.5±0.1	0.5±0.1	6.9, 8.75, 10.6	18.9

We also revised the Introduction to limit the interpretation of the residuals (Revised manuscript, lines 72-80):

"*Because strong mixing can obscure local relationships between AOU and nutrient, residual nutrient diagnostics can be particularly useful in stratified oligotrophic systems, where water masses are more clearly resolved. Residual preformed nitrate ($rPreNO_3$) and residual preformed phosphate ($rPrePO_4$) can be used to evaluate whether measured nutrient inventories are consistent with the regeneration predicted from AOU under parameterized dissolved organic matter (DOM) and particulate organic matter (POM) remineralization (Letscher and Villareal, 2018). Although dependent on the chosen parameters, these residuals can identify deviations from the preset relationship.*"

In the revised Results, their distributions are reported objectively (Revised manuscript, lines 276-283):

"*The ensemble mean $rPreNO_3$ and $rPrePO_4$ values increased progressively from surface through intermediate to deep waters. Positive ensemble mean residuals were observed in the surface NPTSW and ESW, followed by higher values in intermediate waters and maxima in deep waters, where their spatial distributions were relatively homogeneous (Figs. 3d, e). Although the absolute magnitudes of the residuals varied among the 27 parameterizations, the main vertical pattern remained consistent across the parameter ensemble. The corresponding ranges and summary statistics are available in the public data set (Tian, 2026).*

In addtion, we realized that that ensemble averaging does not eliminate the dependence of the

residuals on the transferred empirical parameters based on the reviewers' comments. Therefore, we have revised their role in the interpretation of our results. The low AOU/DIN and AOU/DIP slopes are derived directly from the measured AOU and nutrient concentrations and constitute the observational basis for the reported deviations in oxygen–nutrient coupling. The $rPreNO_3$ and $rPrePO_4$ distributions are used as complementary diagnostics of departures from the prescribed DOM and POM remineralization parameterizations, rather than as independent evidence for the TEP-related or microbial mechanisms proposed in the Discussion. In contrast, they are used together with the directly observed AOU–DIN and AOU–DIP relationships, TEP distributions, and microbial observations to interpret the processes associated with the stoichiometric deviations (Revised manuscript, lines 368-398):

"*The low AOU/DIN and AOU/DIP slopes in the upper and intermediate waters indicate greater nutrient accumulation per unit increase in AOU than expected from the classical reference ratios. Limited vertical nutrient supply maintains persistently oligotrophic conditions in the upper water column (Chl-a in the deep chlorophyll maximum: 0.19−0.31 μg* L^{-1}*). Under nutrient limitation, phytoplankton may allocate a relatively large proportion of photosynthetically fixed carbon to extracellular polysaccharides and TEP with high C:N ratios rather than to nutrient-rich cellular biomass (Curran et al., 2025; Smyth and Letscher, 2023). The observed high TEP-C/POC ratio in the upper 0–300 m (mean of 43.81 ± 14.62%) are consistent with this pattern of carbon allocation (Fig. 3i, Table S1). Positive ensemble average* $rPreNO_3$ *and* $rPrePO_4$ *residuals occurred together with elevated TEP concentrations in the upper water column (Figs. 3d, e, and i). This indicates that measured nutrient concentrations were higher than predicted from AOU under the prescribed DOM and POM remineralization parameters, resulting in a lower AOU/nutrient ratio in the upper waters. Furthermore, evidence indicates that heterotrophic microorganisms preferentially consume components with low C/N ratios, such as proteins, in organic matter during aerobic respira (Curran et al., 2025; Smyth and Letscher, 2023). efore, in the middle water mass, preferential degradation of relatively nutrient rich and labile organic components may enhance nutrient regeneration relative to bulk organic carbon oxidation, thereby contributing to the low AOU/nutrient slopes (Fig. 5a, b). In the deep water mass, the absence of significant*

AOU/nutrients relationships precludes the calculation of meaningful remineralization ratios. In this depth horizon, AOU remains relatively stable whereas nutrient concentrations continue to increase, suggesting that their distributions are governed primarily by the cumulative effects of water-mass aging, lateral transport, and diverse biogeochemical transformations operating on different timescales. Among these, nitrification mediated by ammonia-oxidizing archaea such as Nitrosopumilus may consume oxygen without concomitant phosphorus regeneration (Martens-Habbena et al., 2009), while DOP hydrolysis associated with Alteromonas may mobilize phosphate independently of bulk organic matter oxid (Martens-Habbena et al., 2009), Collectively, these processes likely contribute to the observed decoupling between AOU and nutrients in the deep ocean."

2. Distinguishing whole-water-column observations from layer-specific mechanisms

According to the authors' own results, statistically significant AOU–nutrient relationships are observed only in the upper (0–300 m) and intermediate (300–1000 m) water masses, whereas no significant relationships exist below 1000 m ($p > 0.05$). I therefore recommend that the authors more clearly distinguish between the statistical patterns derived from the entire water column and the mechanisms operating within individual water masses.

If the proposed TEP-driven mechanism is intended to explain the low AOU/nutrient ratios throughout the entire water column, additional evidence is needed to demonstrate that its influence extends from the surface into the mesopelagic and deeper waters. Conversely, if the mechanism is primarily intended to explain the upper ocean, the corresponding statements in the Abstract, Discussion, and Conclusions should be moderated accordingly. In particular, a mechanism fundamentally linked to surface phytoplankton production should not be directly extrapolated to the deep ocean, especially where no statistically significant AOU–nutrient relationships are observed.

Furthermore, it should be noted that the production of TEP and the degradation of TEP are two distinct biogeochemical processes that are expected to have different, and potentially opposite, effects on AOU/nutrient stoichiometry. Current understanding suggests that TEP is produced predominantly within the euphotic zone by phytoplankton, whereas TEP observed

in mesopelagic waters mainly represents exported material undergoing degradation rather than in situ production. The manuscript would therefore benefit from explicitly distinguishing between surface TEP production and subsurface TEP remineralization when discussing the mechanisms responsible for the observed AOU/nutrient ratios. This distinction is particularly important because TEP production and TEP degradation may influence AOU/nutrient stoichiometry in different directions.

Response: We sincerely thank the reviewer for this constructive comment. Based on the reviewers' suggestions, we differentiated the statistical relationships between AOU and nutrients and the mechanisms explaining these relationships according to water masses at different depths, rather than extrapolating to the entire water column. Specifically:

In the upper waters (0–300 m), where significant AOU to nutrient relationships and elevated TEP concentrations were observed, we now restrict the proposed mechanism to phytoplankton production of carbon rich TEP under chronic nutrient limitation. This process can decouple carbon fixation and oxygen production from nitrogen and phosphorus assimilation and thereby contribute to the low AOU to nutrient slopes in the upper ocean.

In the intermediate waters (300–1000 m), we distinguish the transformation of exported organic matter from TEP production in the euphotic zone. Based on evidence that microorganisms preferentially degrade relatively labile substrates with lower C:N ratios (e.g., proteins) (Hwang et al., 2006; Tian et al., 2025), we propose that selective remineralization enhances nutrient release relative to oxygen consumption and contributes to the low AOU to nutrient slopes in these waters.

Below 1000 m, no significant AOU to nutrient relationships were observed. We therefore no longer extend the surface TEP mechanism to the deep waters. Instead, the deep water decoupling is discussed in relation to water mass aging, transport, and additional microbial and geochemical processes that affect oxygen consumption and nutrient accumulation.

We have revised the abstract, discussion, and conclusion sections accordingly:

Revised text in the Abstract (Revised manuscript, lines 14-33):

"*In oligotrophic oceans, the stoichiometric ratios of apparent oxygen utilization (AOU) to nutrients often deviate from the classical Redfield ratio, yet the mechanisms remain poorly constrained. Contrary to the commonly held view that these ratios are typically elevated, we found that the mean ratios of AOU to dissolved inorganic nitrogen (DIN) and AOU to dissolved inorganic phosphorus (DIP) over the upper 2000 m of the oligotrophic Northwest Pacific are only 6.28 and 86.79, respectively, both below the classical values of 8.6 and 138. Strong stratification indicates that physical mixing alone cannot explain these integrated patterns, while depth-resolved regressions further reveal distinct controls among water masses. In upper waters (0–300 m), nutrient limitation promotes phytoplankton to produce TEPs with high C:N ratios, decoupling carbon fixation from nutrient assimilation, a process in which Pelagibacter may play a key role in recycling small organic molecules. In middle waters (300–1000 m), preferential degradation of low C:N compounds within sinking organic matter enhances nutrient regeneration relative to oxygen consumption. Below 1000 m, AOU/nutrient relationships are not statistically significant, indicating that oxygen consumption and nutrient accumulation become increasingly decoupled; this decoupling is likely influenced by Alteromonas activity in polymer degradation and phosphorus mobilization, alongside archaeal nitrification. These findings suggest that biogeochemical models should account for such biological feedbacks to improve predictions of ocean carbon export and nutrient cycling under future climate scenarios.*"

Revised text in the Discussion (Revised manuscript, lines 362-398):

"*To examine how these biogeochemical processes vary across water masses, we calculated AOU/nutrient regression slopes separately for the upper, middle (300−1000 m), and deep water masses (Fig. 5). The AOU/DIN value is lowest in the upper water mass (6.87), increases in the middle water mass (7.21), and becomes statistically insignificant in the deep water mass ($p > 0.05$) (Fig. 5a). The AOU/DIP slopes follow a consistent pattern: lowest in the upper water mass (103.17), increasing in the middle water mass (116.04), and non-significant in the deep water mass (Fig. 5b). The low AOU/DIN and AOU/DIP slopes in the upper and intermediate waters indicate greater nutrient accumulation per unit increase in AOU than expected from the classical reference ratios. Limited vertical nutrient supply*

maintains persistently oligotrophic conditions in the upper water column (Chl-a in the deep chlorophyll maximum: 0.19−0.31 μg L^{-1}). Under nutrient limitation, phytoplankton may allocate a relatively large proportion of photosynthetically fixed carbon to extracellular polysaccharides and TEP with high C:N ratios rather than to nutrient-rich cellular biomass (Curran et al., 2025; Smyth and Letscher, 2023). The observed high TEP-C/POC ratio in the upper 0–300 m (mean of 43.81 ± 14.62%) are consistent with this pattern of carbon allocation (Fig. 3i, Table S1). Positive ensemble average $rPreNO_3$ and $rPrePO_4$ residuals occurred together with elevated TEP concentrations in the upper water column (Figs. 3d, e, and i). This indicates that measured nutrient concentrations were higher than predicted from AOU under the prescribed DOM and POM remineralization parameters, resulting in a lower AOU/nutrient ratio in the upper waters. Furthermore, evidence indicates that heterotrophic microorganisms preferentially consume components with low C:N, such as proteins, in organic matter during aerobic respiration (Hwang et al., 2006; Tian et al., 2025). Therefore, in the middle water mass, preferential degradation of relatively nutrient rich and labile organic components may enhance nutrient regeneration relative to bulk organic carbon oxidation, thereby contributing to the low AOU/nutrient slopes (Fig. 5a, b). In the deep water mass, the absence of significant AOU/nutrients relationships precludes the calculation of meaningful remineralization ratios. In this depth horizon, AOU remains relatively stable whereas nutrient concentrations continue to increase, suggesting that their distributions are governed primarily by the cumulative effects of water-mass aging, lateral transport, and diverse biogeochemical transformations operating on different timescales. Among these, nitrification mediated by ammonia-oxidizing archaea such as Nitrosopumilus may consume oxygen without concomitant phosphorus regeneration (Martens-Habbena et al., 2009), while DOP hydrolysis associated with Alteromonas may mobilize phosphate independently of bulk organic matter oxidation (Saavedra et al., 2025). Collectively, these processes likely contribute to the observed decoupling between AOU and nutrients in the deep ocean."

References:

Hwang, J., Druffel, E. R. M., Eglinton, T. I.,Repeta, D. J.: Source(s) and cycling of the nonhydrolyzable organic fraction of oceanic particles, Geochim. Cosmochim. Acta. 70(20), 5162-5168, https://doi.org/10.1016/j.gca.2006.07.020, 2006.

Tian, D., Li, X., Song, J., Ma, J., Yuan, H.,Duan, L.: Biogeochemical layering and transformation of particulate organic carbon in the Tropical Northwestern Pacific Ocean inferred from $\delta^{13}C$, Ocean Sci., 21(4), 1627-1639, https://doi.org/10.5194/os-21-1627-2025, 2025.

Revised text in the Conclusions (Revised manuscript, lines 524-542):

"*The oligotrophic tropical Northwest Pacific is characterized by pronounced vertical stratification, which retains nutrients at depth and sustains chronic nutrient limitation in the upper ocean. In surface waters, phytoplankton respond to nutrient stress by producing carbon rich transparent exopolymer particles, altering the balance among carbon fixation, oxygen production, and nutrient assimilation. In middle waters, selective transformation of labile and nutrient rich components promotes nitrogen and phosphorus regeneration while carbon rich polysaccharides persist longer. These depth dependent changes are accompanied by shifts in microbial function, with Pelagibacter contributing to the recycling of small organic molecules in upper waters and Alteromonas participating in polymer degradation and potentially in phosphorus regeneration through alkaline phosphatase activity at greater depths. Below 1000 m, the absence of significant AOU to nutrient relationships indicates that nutrient accumulation is increasingly influenced by water mass aging, additional microbial and geochemical processes. The low integrated AOU/DIN and AOU/DIP slopes of 6.28 and 86.79 therefore reflect the combined effects of distinct processes operating among water masses. These findings show that vertical changes in organic matter production, export, and microbial transformation can substantially modify nutrient regeneration stoichiometry and should be considered when representing carbon and nutrient cycling in oligotrophic ocean models.*"

3. Strength of the evidence linking TEP to the observed AOU/nutrient ratios

Another issue concerns the interpretation of the TEP observations. Based on the reported concentrations, the TEP levels observed in this study are generally within the low to moderately low range compared with those reported from the global ocean. Even within the oligotrophic western tropical North Pacific, the measured concentrations appear to be lower than those reported in previous studies, and they are substantially lower than those typically observed in productive coastal regions, frontal systems, or the surface Southern Ocean. Therefore, the statement that TEP-related process is responsible for the observed low

AOU/nutrient ratios should be made with greater caution.In other words, the manuscript currently assumes that TEP abundance is the principal driver of the stoichiometric deviation, yet the observational evidence demonstrates only the presence of TEP rather than an exceptional accumulation relative to other oceanic regions. Therefore, the authors should better justify why relatively modest TEP concentrations are sufficient to produce measurable deviations in AOU/nutrient stoichiometry. Alternatively, the discussion could place greater emphasis on the quality, composition, or turnover of TEP, rather than its absolute concentration, as these characteristics may be more directly linked to remineralization stoichiometry than concentration alone.

Response: We thank the reviewer for this important comment. Although the TEP concentrations in the upper 0–300 m of our study area, ranging from 7.53 to 34.22 μg Xeq L^{-1} with a mean of 22.52 ± 8.54 μg Xeq L^{-1}, were within the low range of published oceanic values. However, the relative contribution of TEP to the small particulate carbon pool was substantial. TEP-C accounted for 15.45–71.75% of POC, with a mean contribution of 43.81 ± 14.62%, which was generally higher than those observed in most productive coastal, shelf, and open ocean environments. Thus, the relevant feature of our observations is not exceptional TEP accumulation in absolute terms, but the relatively large contribution of TEP to POC. To provide a more balanced assessment, we have added a new supplementary table (Table 2/Revised Table S1) comparing TEP concentrations and TEP-C/POC ratios from this study with those reported for oligotrophic open-ocean waters, productive coastal systems, frontal regions, and the surface Southern Ocean. All TEP-C/POC values were standardized using a conversion factor of 0.51 based on Engel and Passow (2001).

Accordingly, we have revised the description of TEP absolute abundance in the Introduction (Revised manuscript, lines 98-100):

"*Although their absolute concentrations are often low in oligotrophic oceans, TEP can constitute a substantial fraction of the small POC pool and can be abundant relative to the low phytoplankton biomass (Kodama et al., 2014; Zamanillo et al., 2019).*"

Reference:

Zamanillo, M., Ortega-Retuerta, E., Nunes, S., Rodríguez-Ros, P., Dall'Osto, M., Estrada, M., et al.: Main drivers of transparent exopolymer particle distribution across the surface Atlantic Ocean, Biogeosciences., 16(3), 733-749, https://doi.org/10.5194/bg-16-733-2019, 2019.

And we have revised the Results to include a description of the TEP-C/POC ratio (Revised manuscript, lines 276-283, 294-304):

"*The ensemble mean $rPreNO_3$ and $rPrePO_4$ values increased progressively from surface through intermediate to deep waters. Positive ensemble mean residuals were observed in the surface NPTSW and ESW, followed by higher values in intermediate waters and maxima in deep waters, where their spatial distributions were relatively homogeneous (Figs. 3d, e). Although the absolute magnitudes of the residuals varied among the 27 parameterizations, the main vertical pattern remained consistent across the parameter ensemble. The corresponding ranges and summary statistics are available in the public data set (Tian, 2026).*

POC and TEP exhibit a distribution pattern that is nearly opposite to that of nutrients and DIC among the different water masses (Figs. 3g, h, i). TEP concentrations in the upper water ranged from 7.53 to 34.22 μg Xeq L^{-1} (mean 22.52 ± 8.54 μg Xeq L^{-1}), exceeding those in deeper waters. These concentrations were within the low range reported for open ocean environments (Table S1). Nevertheless, when TEP concentrations were converted to estimated carbon equivalents using a factor of 0.51 (Engel and Passow, 2001), the TEP-C/POC ratio ranged from 15.45% to 71.75%, with a mean of 43.81 ± 14.62%, which was generally higher than those observed in most productive coastal, shelf, and surface open ocean (Table S1). Therefore, the estimated TEP-associated carbon was substantial relative to the measured POC pool, despite the modest absolute TEP concentrations."

Reference:

Engel, A.,Passow, U.: Carbon and nitrogen content of transparent exopolymer particles (TEP) in relation to their Alcian Blue adsorption, Mar. Ecol. Prog. Ser., 219, 1-10, https://doi.org/10.3354/meps219001, 2001.

Table 2/Revised Table S1. Comparison of TEP concentrations and TEP-C/POC ratios in the upper ocean

Region	Depth	TEP concentration (μg Xeq L^{-1})	TEP-C/POC (%)	Reference
*Tropical Northwest Pacific	0–300 m	7.53–34.22 (22.52 ± 8.54)	15.45–71.75 (43.81 ± 14.62)	This study
Fram Strait	5-150 m	5–517 (75 ± 78)	13.8 ± 6.1	Engel et al. (2017)
Northern South China Sea	0–200 m	0.6–78.6	5.6–55.5 (27.4 ± 1.3)	Ge et al. (2022)
*South China Sea	0–220 m	14–47 (30 ± 8)	32.0–173 (75.0 ± 37.0)	Guo et al. (2022)
*Western tropical North Pacific	0–220 m	12–54 (34 ± 10)	45.0–114 (61.0 ± 40.0)	Guo et al. (2022)
Jaran Bay	Subsurface	26.5–1695.4 (215.9 ± 172.2)	2.4–67.3 (21.7 ± 11.4)	Lee et al. (2020)
East China Sea coast	Surface	11.25–509.58 (214.90)	30.2	Wen et al. (2022)
North of the South Orkney Islands	Surface	144.4 ± 21.7	45.9 ± 5.1	Zamanillo et al. (2019a)
South of the South Orkney Islands	Surface	48.1 ± 6.5	40.8 ± 10.2	Zamanillo et al. (2019a)
Northwest of South Georgia	Surface	125.5 ± 21.1	30.6 ± 5.1	Zamanillo et al. (2019a)
West of Anvers Island	Surface	111.6 ± 13.0	25.5 ± 5.1	Zamanillo et al. (2019a)
*Open Atlantic Ocean	Surface	18.3–131.7 (59.8 ± 27.4)	34.0–103 (66.0 ± 19.0)	Zamanillo et al. (2019b)
Southwestern Atlantic Shelf	Surface	98.6–427.2 (255.7 ± 130.4)	28.0–110 (73.0 ± 36.0)	Zamanillo et al. (2019b)

*Oligotrophic ocean; A factor of 0.51 was used to convert TEP (μg Xeq L^{-1}) to TEP-C (μg C L^{-1}) (Engel and Passow, 2001).

References:

Engel, A.,Passow, U.: Carbon and nitrogen content of transparent exopolymer particles (TEP) in relation to their Alcian Blue adsorption, Mar. Ecol. Prog. Ser., 219, 1-10, https://doi.org/10.3354/meps219001, 2001.

Engel, A., Piontek, J., Metfies, K., Endres, S., Sprong, P., Peeken, I., et al.: Inter-annual variability of transparent exopolymer particles in the Arctic Ocean reveals high sensitivity to ecosystem changes, Scientific Reports. 7(1), 4129, https://doi.org/10.1038/s41598-017-04106-9, 2017.

Ge, Z., Li, Q. P., Yang, W., Liu, X.,Wu, Z.: Transparent exopolymer particle dynamics along a shelf-to-sea gradient and impacts on the regional carbon cycle, Science of The Total Environment. 808, 152117, https://doi.org/10.1016/j.scitotenv.2021.152117, 2022.

Guo, S., Wu, Y., Zhu, M.,Sun, X.: Concentrations of transparent exopolymer particles (TEPs) and their role in the carbon export in the South China Sea and western tropical North Pacific, Marine Environmental Research. 179, 105699, https://doi.org/10.1016/j.marenvres.2022.105699, 2022.

Lee, J. H., Lee, W. C., Kim, H. C., Jo, N., Jang, H. K., Kang, J. J., et al.: Transparent Exopolymer Particle (TEPs) Dynamics and Contribution to Particulate Organic Carbon (POC) in Jaran Bay, Korea, Water. 12(4), 1057, https://doi.org/10.3390/w12041057, 2020.

Wen, L., Li, X., Song, J.,Ma, J.: Transparent exopolymer particle (TEP) and its impact on marine carbon transport along the East China Sea coast, Ecological Indicators. 137, 108791, https://doi.org/10.1016/j.ecolind.2022.108791, 2022.

Zamanillo, M., Ortega-Retuerta, E., Nunes, S., Estrada, M., Sala, M. M., Royer, S. J., et al.: Distribution of transparent exopolymer particles (TEP) in distinct regions of the Southern Ocean, Science of The Total Environment. 691, 736-748, https://doi.org/10.1016/j.scitotenv.2019.06.524, 2019a.

Zamanillo, M., Ortega-Retuerta, E., Nunes, S., Rodríguez-Ros, P., Dall'Osto, M., Estrada, M., et al.: Main drivers of transparent exopolymer particle distribution across the surface Atlantic Ocean, Biogeosciences. 16(3), 733-749, https://doi.org/10.5194/bg-16-733-2019, 2019b.

We have also restructured the Discussion to address the causes of deviations in AOU/nutrient stoichiometry separately for different depth layers, thereby avoiding any implication that TEP abundance alone is the primary driver (See the reply to major comment 2 for details).

Minor or specific:

1. The reported analytical precision of the POC measurements deserves further clarification. In general, the instrumental precision of an elemental analyzer for carbon determination is typically on the order of approximately 1% under routine laboratory conditions. For real samples, however, the overall analytical precision is usually lower because additional uncertainties are introduced during sample collection, filtration, acidification (or acid

fumigation), drying, and other pretreatment procedures. Therefore, the reported analytical precision of 0.8‰ appears to be exceptionally high—nearly two orders of magnitude better than the analytical precision commonly achieved in routine laboratory measurements of marine suspended particulate organic carbon. I am therefore curious about how this level of precision was achieved. Does this value refer to the repeatability of the elemental analyzer itself, the precision of repeated analyses of laboratory standards, or the overall analytical precision including sample pretreatment? Alternatively, could this simply be a typographical error? I recommend that the authors clarify how this value was determined and what it specifically represents.

Response: We thank the reviewer for identifying this issue. After reexamining the analytical procedure and the cited methods, we found that the reported value of ±0.8‰ was inappropriately expressed and did not represent the overall precision of POC determination. Because full process replicate field samples were unavailable, the overall method precision, including uncertainties associated with filtration, acid treatment, drying, and instrumental measurement, could not be independently quantified. We have therefore removed the ±0.8‰ value. The revised Methods are as follows (Revised manuscript, lines 180-185):

"*The pretreated samples were analyzed for POC concentration using an elemental analyzer (Thermo Fisher Scientific Flash EA 1112, United States). Carbon quantification was calibrated using standard reference materials, including USGS64 (C % = 31.97 %, Indiana University), USGS40 (C % = 40.8 %, U.S. Geological Survey), and Urea #2a (C % = 20 %, Indiana University), which were also used to monitor instrument performance (Ma et al., 2021b).*"

2. The description of the TEP analytical method requires clarification. The current protocol omits several key steps of the standard Alcian Blue assay (e.g., staining and washing), making it unclear whether the standard method was actually followed or whether these procedures were inadvertently omitted from the manuscript. In addition, the authors should clarify whether the xanthan gum calibration curve was established under their own experimental conditions or directly adopted from Bittar et al. (2018), as calibration curves are generally expected to be generated within each laboratory to ensure quantitative reliability.

Response: We thank the reviewer for pointing out these important issues regarding the TEP analytical method. The staining and rinsing steps were performed during sample collection and were described in Sect. 2.1 (original manuscript, lines 139-144): "*TEP samples were collected by filtering 1−4 L of seawater through polycarbonate filters (0.45 µm pore size, Whatman) under a vacuum of 170 mmHg. The filtered membrane was stained with 0.5−1 mL of a 400 mg L^{-1} Alcian Blue solution (Sigma-Aldrich, USA) for 5−10 s, rinsed with 5 mL of MilliQ water, and stored at -20 °C until measurement (three replicate samples were collected at each depth).*" Because the sampling procedure and the laboratory analysis were presented in separate subsections, the complete method may not have been immediately evident. In addition, the pH of the Alcian Blue solution was omitted from the original manuscript. We have now added that the staining solution was adjusted to pH 2.5 with glacial acetic acid. This information has now been added to the revised Methods (Revised manuscript, lines 146-149):

"*The retained particles were stained with 0.5−1 mL of a 400 mg L^{-1} Alcian Blue solution (Sigma-Aldrich, USA) for 5−10 s, prepared in Milli Q water and acidified to pH 2.5 with glacial acetic acid. The filters were then rinsed with 5 mL of MilliQ water, and stored at -20 °C until measurement.*"

Regarding the calibration curve, we appreciate the reviewer's concern. Our original wording may have inadvertently implied that we directly adopted the calibration curve from Bittar et al. (2018). In fact, the updated procedure described by Bittar et al. (2018) was used only as a methodological reference for establishing the xanthan gum calibration curve, and the calibration curve was independently generated in our laboratory under our own experimental conditions. To avoid any ambiguity, we have revised the TEP analysis subsection to explicitly state that the xanthan gum calibration curve was prepared specifically for this study following the protocol of Bittar et al. (2018), with the absorbance converted to xanthan gum equivalents (Xeq) weight using this laboratory-generated calibration curve (Figure 1/Revise Figure S1). The relevant calibration curve and supplementary method description are detailed in the supplementary materials (Supplementary material; lines 20-33):

"*A fresh xanthan gum stock solution (75 mg L^{-1}) was diluted to obtain five standards. Aliquots of 0.125, 0.250, 0.500, 0.750, and 1.000 mL of the stock solution were pipetted into clean 5*

mL polypropylene tubes, and the final volume of each standard was adjusted to 1 mL with ultrapure water. This produced standards containing 9.37, 18.75, 37.50, 56.25, and 75.00 µg xanthan gum, respectively, with three replicates at each level. Each standard was mixed with 0.5−1 mL of Alcian Blue solution (400 mg L^{-1}, pH 2.5) for 5−10 s and filtered through a 0.45 µm polycarbonate membrane (Whatman) under a vacuum below 175 mmHg. Procedural blanks were processed in parallel. The filters were extracted with 6 mL of 80% sulfuric acid for 10 h, and absorbance was measured at 787 nm. A linear regression of xanthan gum mass against absorbance after blank correction yielded:

$$M_{XG} = 100.15A_{787} + 1.67 \quad (1)$$

where M_{XG} is the xanthan gum equivalent mass in µg and A_{787} is the absorbance at 787 nm (R^2=0.99; Fig. S1). TEP concentrations were calculated by dividing the xanthan gum equivalent mass by the filtered seawater volume and are reported as µg Xeq L^{-1}."

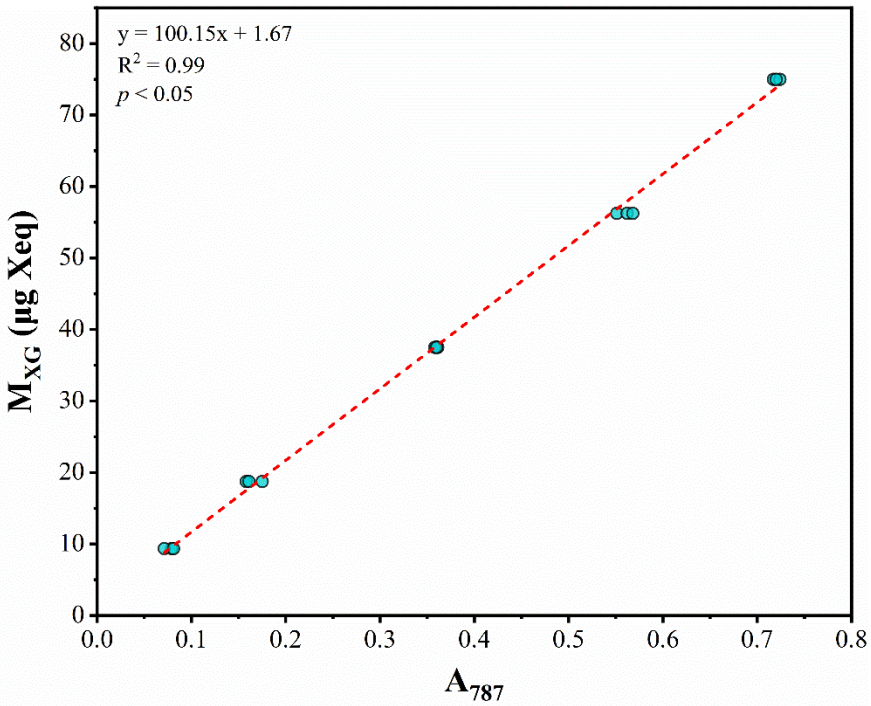

Figure 1/Revise Figure S1. Xanthan gum calibration curve for TEP quantification.

3. What do the red arrows mean in fig 2a?

Response: We thank the reviewer for pointing out this ambiguity. In the original Fig. 2a, the

red arrows with horizontal lines were intended to indicate the boundaries distinguishing different water masses. However, we recognize that this representation was not sufficiently clear and could cause confusion. To improve readability, we have revised the figure by removing the arrows, as the T-S diagram itself, with its characteristic clustering of data points, already allows for clear identification of each water mass without additional markings. We believe this modification makes the figure cleaner and easier for readers to interpret (Figure 2/Revise Figure2).

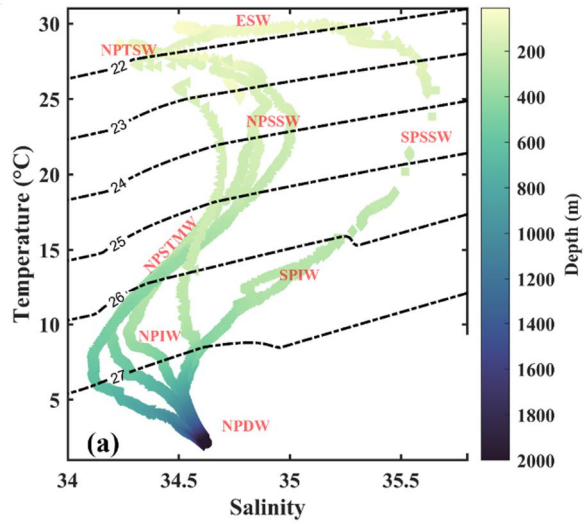

Table 2. Characteristics of water masses in the study area

Water Masses	Temperature (°C)	Salinity (‰)	γ_n (Kg m^{-3})
NPTSW	27.99-29.45 (28.71)	34.29-34.63 (34.45)	21.62-22.58 (21.76)
ESW	29.28-29.87 (29.56)	34.59-35.27 (35.01)	21.44-22.76 (21.89)
SPSSW	19.62-26.64 (22.95)	35.46-35.52 (35.51)	22.93-25.95 (24.25)
NPSSW	18.76-27.04 (23.89)	34.62-34.98 (34.80)	22.59-24.99 (23.51)
NPSTMW	13.23-16.45 (15.00)	34.42-34.68 (34.55)	25.00-26.00 (25.67)
NPIW	3.91-11.16 (7.36)	34.12-34.58 (34.40)	26.01-27.59 (26.99)
SPIW	5.47-12.43 (8.55)	34.52-34.94 (34.65)	26.00-27.40 (26.99)
NPDW	2.05-4.63 (3.07)	34.51-34.63 (34.58)	27.41-27.92 (27.76)

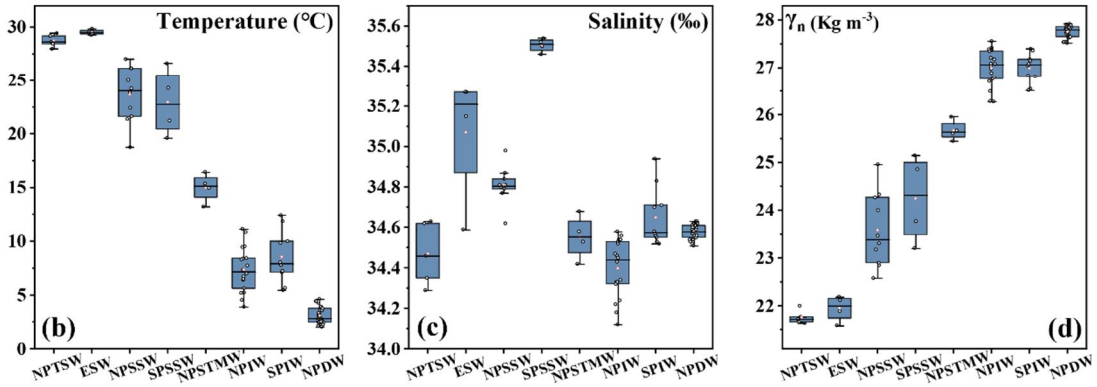

Figure 2/Revise Figure2. Physical properties of water masses in the research area.

We are grateful for your thorough review and constructive suggestions, which have significantly enhanced the quality of our manuscript. We have carefully addressed all of your comments and hope that the revised version now meets the journal's standards. Thank you once again for your time and valuable input.